First experiments with the negative ion source NIO1

M. Cavenago,[1,a)] G. Serianni,[2] M. De Muri,[1,2] P. Agostinetti,[2] V. Antoni,[2] C. Baltador,[2]
M. Barbisan,[2] L. Baseggio,[2] M. Bigi,[2] V. Cervaro,[2] F. Degli Agostini,[2] E. Fagotti,[1]
T. Kulevoy,[1,3] N. Ippolito,[4] B. Laterza,[2] A. Minarello,[1] M. Maniero,[2] R. Pasqualotto,[2]
S. Petrenko,[1,3] M. Poggi,[1] D. Ravarotto,[2] M. Recchia,[2] E. Sartori,[2] M. Sattin,[1] P. Sonato,[2]
F. Taccogna,[4] V. Variale,[4] P. Veltri,[2] B. Zaniol,[2] L. Zanotto,[2] and S. Zucchetti[2]

[1]*INFN-Laboratori Nazionali di Legnaro (LNL), v.le dell'Università 2, I-35020 Legnaro PD, Italy*
[2]*Consorzio RFX, Corso Stati Uniti 4, I-35127 Padova, Italy*
[3]*ITEP, Bolshaja Cheremushkinskaja 25, 110079 Moscow, Russia*
[4]*Istituto Nazionale di Fisica Nucleare, Bari, Italy*

Neutral Beam Injectors (NBIs), which need to be strongly optimized in the perspective of DEMO reactor, request a thorough understanding of the negative ion source used and of the multi-beamlet optics. A relatively compact radio frequency (rf) ion source, named NIO1 (Negative Ion Optimization 1), with 9 beam apertures for a total H^- current of 130 mA, 60 kV acceleration voltage, was installed at Consorzio RFX, including a high voltage deck and an X-ray shield, to provide a test bench for source optimizations for activities in support to the ITER NBI test facility. NIO1 status and plasma experiments both with air and with hydrogen as filling gas are described. Transition from a weak plasma to an inductively coupled plasma is clearly evident for the former gas and may be triggered by rising the rf power (over 0.5 kW) at low pressure (equal or below 2 Pa). Transition in hydrogen plasma requires more rf power (over 1.5 kW). ○

I. INTRODUCTION

Power efficiency of neutral beam injectors for DEMO (DEMOnstration Power Plant) reactor[1,2] and other fusion applications critically depends on component performances, including the multiaperture negative ion sources. The ion source NIO1[3,4] (Negative Ion Optimization 1, nominal H^- beam current of 130 mA at 60 keV, divided into 9 beamlets) built by Consorzio RFX and INFN aims to provide a reduced-size model of these sources and a versatile test bench for innovations and for simulation code validations. The modular design of NIO1 source and accelerator column allowing for replacement of improved parts and electrodes was previously described.[3–5] Recent experiments and improvements are the subject of this paper.

NIO1 is a radio frequency (rf) ion source with an external solenoid antenna (or coil), as the larger sources,[6] like SPIDER[7] (Source for Production of Ion of Deuterium Extracted from RF plasma) under construction for the neutral beam injectors. A $f = \omega/2\pi = 2$ MHz (tunable by $\pm 10\%$) radio frequency generator can provide a forward power P_f up to 2.5 kW in continuous regime, through a standard matching circuit (page 396 in Ref. 8). Energy transfer between rf coil and plasma electrons depends both on e^--gas collisions and on stochastic heating;[8,9] moreover, inductively coupled plasmas (ICP or H-mode) are expected at large P_f and electron density n_e, while capacitive coupling to coil voltage (E-mode) is possible[8,9] at lower density. These aspects are of course relevant to ion source power efficiency, whose study is one of NIO1 goals.

Another goal is to improve beam quality and the models of beam extraction, for which we developed several simulation tools and studies.[10–12] The reduced size of NIO1 respect to SPIDER allows making complete 3D simulations possible, without imposing symmetries or simplifications. The same size ratio makes the NIO1 electrodes more rigid and easier to cool. On the other hand, miniaturization of some NIO1 parts makes construction and monitoring more difficult. Use of NIO1 for beam energy recovery tests is also considered.[13]

First plasmas were obtained in July 2014 using air as a filling gas, while a hydrogen supply gas line was added later. In general, plasma from H_2 requires much more rf power than air does (and irradiates less light[14]). Improvement in used rf power and in cooling continued up to July 2015, when ICP regime (or H mode) was attained also for H_2. A status of the NIO1 installation and improvements is given in Section II. Experiments both with air (where the P_f power range near E–H transition was easily covered by NIO1) and separately H_2 are described in Section III.

II. NIO1 INSTALLATION

Some views of the NIO1 installation are given in Figs. 1 and 2; vacuum chamber sections are the ion source head, the acceleration column, a pump cross, and the diagnostic chamber, with the beam axis z horizontal.[4,5] Acceleration column major electrodes are the plasma grid (PG, nominal voltage -60 kV), the extraction grid (EG, -52 kV) and the post-
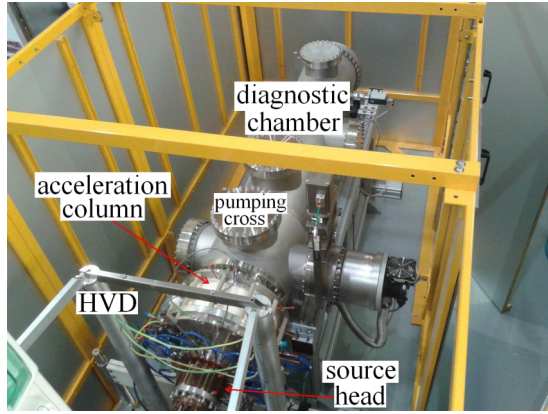
FIG. 1. Overview of NIO1 source, acceleration column, and diagnostic chamber (as labeled); HVD cover removed to make source head visible.

acceleration grid (PA, near ground). The source head is made by several modules, sealed by O-rings, namely, the PG support, the bias plate support, the front multipole, the rf coil module, the rear multipole, and the rear cover. The source head is cantilevered on the PG outer flange and on the accelerator column, which are supported by the pumping cross and an additional support; structure was precisely aligned and successfully put under vacuum in February 2014. The source head is enclosed by a High Voltage Deck (HVD), which supplies cooling and power connection to the ion source. Among others, HVD contains the rf generator, the rf matching box, the gas dosing valve, the low voltage power supplies for a filter field circuit, the bias plate and the source bias, and the HV supply for the EG. Control system and hardware interlock communicate via dedicate fiber optic lines with the operator console. A reasonably extended version of the control and acquisition system is now installed, and in continuous upgrading.

The HVD and the NIO1 vacuum chamber are enclosed by a lead box (area 1.7×4.3 m) with 3 doors, while the 70 kV/50 kVA epoxy insulated transformer powering the HVD is placed in a separated box. A 70 kV/170 mA power supply gives the voltage V_{PG} to the HVD and the PG (and is interlocked to those 3 doors). After some acceleration column conditioning, the HVD holds the rated voltage, with plasma off. The gas feeding line works near atmospheric pressure to

FIG. 2. (a) View of the NIO shielding box with main door open and main rf generator removed; (b) accelerator column and HVD view from the opposite side.

avoid Paschen discharges, its HV breaks are protected with voltage dividers and required long time for construction and approval.

The HV system is now programmed to stop at the first arc (or noise) detection. Beam extraction voltage is so still limited by electronic testing, and commissioning, and in practice, up to now, source plasma was operated at $V_{PG} = 0$. It is expected that beam operation will begin soon but starting with $|V_{PG}| << 60$ kV. A carbon fiber composite (CFC) tile was temporarily installed for tests and beam imaging at low beam power. A view port for beam emission spectroscopy was also installed on NIO1. At the same time, a copper calorimeter,[3] strongly water cooled, is being instrumented before installation. The Fast Emittance Scanner (FES) installation was also delayed, and FES is now being tested in LNL.

Aiming at reproducing long pulses operation condition (>1000 s), NIO1 water cooling system has to be sized for continuous operation and it was recently upgraded to remove about 15 or 20 kW of power.[5] NIO1 plasma is so operated in a continuous regime, up to about 6 h per day. Other items of the cooling system like cooling water resistivity and flow distribution are being improved with use.

In the source head the rear cover has four ports, one used for gas injection, one connected (via a light collector system and a fiber optic) to a calibrated photomultiplier (PMT), another connected a spectrometer, and the fourth one illuminating a luxmeter, with a 0.009 sr view angle at a 0.2 m distance. The PG support has 2 passing viewlines for optical spectroscopy, one CF16 port for Caesium injection and another CF16 port where the pressure p_1 is measured. Let p_2 be the pressure in the diagnostic chamber and V_1 the control voltage of the gas dosing valve. A calibration of p_1, p_2, and V_1 is recorded before each experimental campaign with plasma off. When plasma is on, only p_2 is relied on as a measurement, and the corresponding p_1 inferred by calibration has the meaning of a filling pressure. At low gas load, p_1/p_2 is about 20 for air and 2 for hydrogen (since one turbo only is used and pumping speed S decreases for H_2 and PG conductance increases[11] to $C_1 = 0.1$ m^3/s). It must be noted that the initial NIO1 design called for a (large) total pumping speed $S > 0.5$ m^3/s (or preferably $S > 1$ m^3/s) for H_2 at $p_1 = 1$ Pa (and consequently $p_2 = 0.16$ Pa) providing up to 4 ports (200 mm diameter or more) for pumps. Cost comparison of both traditional (turbomolecular with N_2 purge, cryogenic) and special NEG (Non Evaporable Getter) pumps is in progress.

Source emission spectroscopy[13] (even within the limitation of NIO1 available viewlines) proved to be a useful diagnostic; in particular, a low (1.3 nm) resolution spectrometer was also used for real time plasma monitoring; and together with the luxmeter readout L_x and the PMT signal (converted to a calibrated incident power P_{pmt}), they represented a redundant system for plasma control. A similar spectrometer was recently installed also on the LNL test plasma generator.[3]

As for rf equipment, the matching box is tuned to have an input impedance $Z_1 > 50$ Ω when plasma is off (typically $Z_1 \geq 70$ Ω measured at low voltage); the rf generator was chosen to withstand this condition, which requires a strong water cooling. The actual impedance is not measured during plasma operation, and digital readout (supplied by the rf

generator) of forward P_f and reflected P_r power is filtered (by the control and acquisition system) and recorded. The matching box has two Rogowski coils, which monitor the input and output currents, giving monitor signals V_{in} and V_{out}. During operation with $V_{PG} = 0$, their rms amplitudes are recorded, and in a few cases, signal shapes were analyzed. When plasma is on, noticeable harmonics appear in the input monitor signal V_{in} (the fifth harmonics is -18 dB the fundamental and the third one slightly less). In the output monitor, V_{out} harmonics were less visible, and less than -50 db with respect to the fundamental 2 MHz frequency, which of course is enhanced by the resonance of the matching box and rf coil circuit.

III. EXPERIMENTS

First experiments studied the relation between pressure p_1 and forward rf power P_f, limited to 0.33 kW, and plasma luminosity. With air and $p_1 > 6$ Pa, the threshold power P_o for plasma onset was not measurable (lower than 50 W). After plasma is turned on, plasma can be maintained at lower pressures (1 Pa), with more rf power P_f. Emission spectroscopy data show a large electron temperature ($T_e > 7$ eV with a preliminary analysis) but with large uncertainties due to air impurity and electron energy distribution[4] (and to weak line intensity).

The increasing of power $P_f > 0.3$ kW greatly increased the plasma luminosity, which reduces the integration time needed for spectra acquisition, and a large number of data sets were collected at pressure p_1 ranging from 0.36 Pa to 11.6 Pa, with forward power P_f from 0.3 kW to 0.85 kW, for filling gas air. For pressure $p_1 \leq 2$ Pa, luminosity L_x jumps when increasing P_f over a threshold P_t about 0.55 kW. For example, at $p_1 = 0.9$ Pa, see Fig. 3, L_x rises from 1 Lux to 5 Lux when P_f rises from 0.5 kW to 0.6 kW (and $L_x = 20$ Lux when $P_f = 0.8$ kW); similarly for P_{pmt} and for M_{394}, defined as the photon (ph) density collected in a 0.3 nm bandwidth around wavelength $\lambda = 394$ nm corrected for noise, background, and detection losses.[14] From the ratio of M_{391} (similarly defined)

and M_{394}, using a typical model curve,[15] we can have a preliminary estimate of electron temperature T_e (here named inferred temperature).

Note that Figure 3 data were taken by rising P_f from one point to next. Typically, the luminosity jump has hysteresis, that is, going back to a weak luminosity plasma requires to set P_f well below P_t (say by 20%).

A preliminary analysis of spectrograph data also shows that M_{394} increases from 10^{17} ph s^{-1} m^{-2} to 1.3 $\times 10^{18}$ ph s^{-1} m^{-2} when pressure decreases from $p_1 = 4$ Pa to 0.5 Pa (keeping $P_f = 0.5$ kW); at the same time, the inferred electron temperature T_e goes from about 9 eV (over 2 Pa) to 4 eV (below 1 Pa), within 10% error, see Fig. 4. To avoid possible ambiguities due to hysteresis, data for this picture were selected with the following procedure. For each value of the pressure p_2 under study, rise P_f in small steps (from a low value to values well above P_t); at each step stabilize p_2 if needed, then verify P_f and record reflected power P_r, spectra and any other plasma information; then continue study with another pressure; off-line, data points with net rf power $P = P_f - P_r$ equal to 0.47 kW within 10 W were grouped, and p_2 converted to p_1 with known calibration.

Similar results for plasma luminosity[3] and similar spectra were obtained for a test plasma generator at LNL (plasma chamber radius 60% of NIO1), at scaled rf power (transition about 0.25 W) where both air or pure nitrogen was available as feeding gases.

Data points with larger inferred electron temperatures (correlated to weaker luminosity) can be considered as an indication of E-mode, also in the NIO1 case, while the brighter plasma (with about $T_e = 4$ eV) corresponds to inductive coupling (H-mode). Since NIO1 has no Faraday shield, sharp E–H mode transitions are expected. As a remark, comparing data taken in 4 different days on NIO1, some increase of threshold P_t is apparent (from 0.45 to 0.55 kW), which requires further investigations.

Experiments (especially scan of P_f) with hydrogen[14] as a filling gas up to now covered a smaller pressure range, p_1 from 0.5 Pa to 3 Pa at a necessarily wider power scan, P_f from 0.1 up
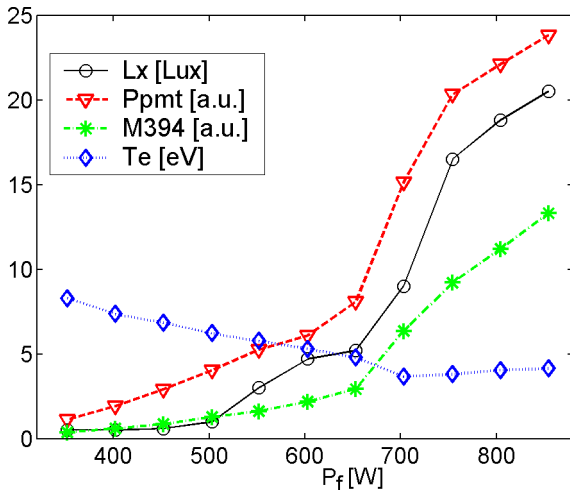
FIG. 3. Plasma luminosity L_x vs forward rf power P_f at $p_1 = 0.9$ Pa (air), also shown P_{pmt} (1 a.u. = 10 mW), M_{394} (1 a.u. = 10^{17} ph s^{-1} m^{-2}), and T_e; typical error $\pm$ 10%.
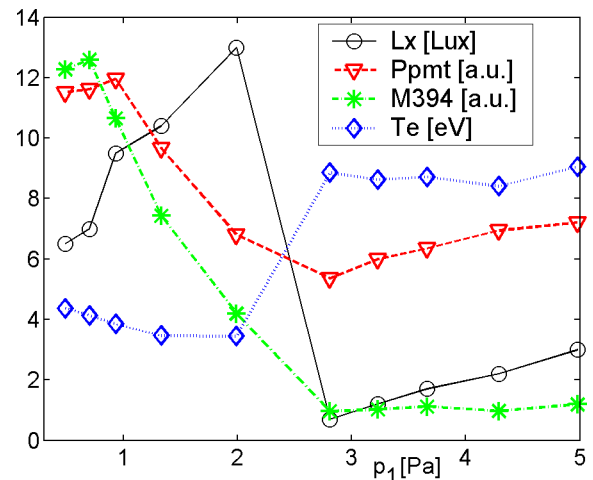
FIG. 4. Plasma luminosity L_x vs source pressure p_1 (air) at constant net rf power $P = P_f - P_r = 0.47$ kW; P_{pmt}, M_{394}, and T_e as in Fig. 3; typical error $\pm$ 10%.
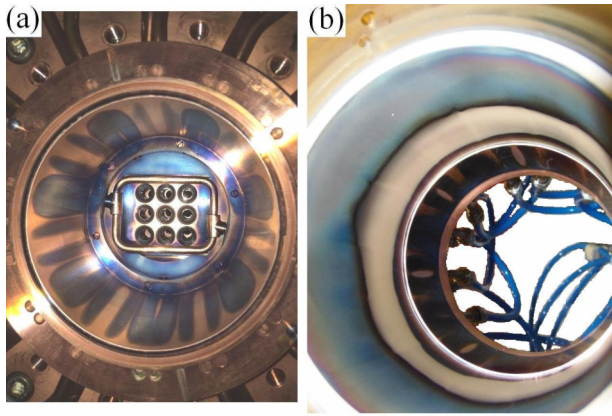
FIG. 5. (a) The front multipole with bias plate and PG beam extraction holes; (b) the rf coil module with the rear multipole attached.

to 1.7 kW. A vacuum loss appeared after continuous operation at 1.7 kW; no air contamination is evident in collected spectra before this occurrence. Only major features are here noted. First, power for plasma onset P_o was noticeable, about $P_o = 200$ W at $p_1 = 2.6$ Pa. Second, luxmeter readout was rarely over the noise level ($L_x > 0.5$ Lux) until $P_f > 1.3$ kW; brilliance integrated from the low resolution spectrometer data[14] or P_{pmt} was correspondingly lower than for air plasma; electron temperature T_e (inferred from other spectral lines and models[14,15]) does not show large discontinuities (vs P_f or p_1). Rising power up from 1.4 to 1.7 kW for $p_1 = 2.4$ Pa resulted in a significant rise in L_x (from 0.5 to 4.5 Lux) and in P_{pmt} (from 25 mW to 64 mW) which are consistent with inductively coupled plasma (as seen for air). Anyway, the plasma behavior for $P_f < 1.5$ kW may be a mixture of E and H modes. Explanation may be simply circumstantial: dismounting the ion source head (rear multipole and rf coil module, see Fig. 5(b)), some wall sputtering was apparent; rf window was covered by rings of deposited material, at both ends, separated by a 29 mm height clean surface (rings height about 10 and 38 mm, with a resistance between diametrically opposed pads of 146 Ω and 15 Ω, respectively). It is planned to continue experiments with a new clean rf window, with a better cooling and an improved sealing procedure; some protection of source metallic walls with Mo liners is also considered.

The existence of an E–H mode transition is an important input for numerical and analytical modelling of ion sources; moreover, implying that a model that assumes H mode coupling (see Ref. 16 for a review of ICP) should be not directly compared to data taken in a source without Faraday shield at very low rf power, where capacitive coupling may be dominant. Several diagnostic signatures,[3] useful for E–H mode distinction, were here confirmed. I n s ummary, NIO1 experiments with air (as filling gas) have evidenced important features of this E–H mode transition in a cylindrical geometry, with similarities to the more complicated case of hydrogen, where interesting preliminary results were also obtained.

[1]H. Zohm, C. Angioni, E. Fable, G. Federici, G. Gantenbein, T. Hartmann, K. Lackner, E. Poli, L. Porte, O. Sauter, G. Tardini, D. Ward, and M. Wischmeier, Nucl. Fusion 53, 073019 (2013).

[2]M. Honda, T. Takizuka, K. Tobita, G. Matsunaga, and A. Fukuyama, Nucl. Fusion 51, 073018 (2011).

[3]M. Cavenago, T. Kulevoy, S. Petrenko, G. Serianni, V. Antoni, M. Bigi, F. Fellin, M. Recchia, and P. Veltri, Rev. Sci. Instrum. 83, 02A707 (2012).

[4]M. Cavenago, G. Serianni, V. Antoni, M. Bigi, M. De Muri, R. Pasqualotto, M. Recchia, P. Veltri, P. Agostinetti, M. Barbisan, L. Baseggio, V. Cervaro, M. Cazzador, F. Degli Agostini, L. Franchin, T. Kulevoy, B. Laterza, A. Mimo, A. Minarello, S. Petrenko, D. Ravarotto, F. Rossetto, M. Sattin, B. Zaniol, and S. Zucchetti, AIP Conf. Proc. 1655, 040006 (2015).

[5]M. de Muri, M. Cavenago, G. Serianni, P. Veltri, M. Bigi, R. Pasqualotto, M. Barbisan, M. Recchia, B. Zaniol, T. Kulevoy, S. Petrenko, L. Baseggio, V. Cervaro, F. Degli Agostini, L. Franchin, B. Laterza, A. Minarello, F. Rossetto, M. Sattin, and S. Zucchetti, Fusion Eng. Des. 96-97, 249 (2015).

[6]W. Kraus, U. Fantz, P. Franzen, M. Fröschle, B. Heinemann, R. Riedl, and D. Wünderlich, Rev. Sci. Instrum. 83, 02B104 (2012).

[7]P. Agostinetti, V. Antoni, M. Cavenago, G. Chitarin, N. Marconato, D. Marcuzzi, N. Pilan, G. Serianni, P. Sonato, P. Veltri, and P. Zaccaria, Nucl. Fusion 51, 063004 (2011).

[8]M. A. Lieberman and A. J. Lichtenberg, Principles of Plasma Discharges and Material Processing (John Wiley, New York, 1994).

[9]St. Lishev, A. Shivarova, Kh. Tarnev, S. Iordanova, I. Koleva, Ts. Paunska, and D. Iordanov, J. Phys. D: Appl. Phys. 46, 165204 (2013).

[10]N. Fonnesu, M. Cavenago, G. Serianni, and P. Veltri, Rev. Sci. Instrum. 87, 02B905 (2016).

[11]E. Sartori, P. Veltri, M. Cavenago, and G. Serianni, Rev. Sci. Instrum. 87, 02B118 (2016).

[12]F. Taccogna, P. Minelli, M. Cavenago, P. Veltri, and N. Ippolito, "The characterization and optimization of NIO1 ion source extraction aperture using a 3D particle-in-cell code," Rev. Sci. Instrum. (these proceedings).

[13]V. Variale, M. Cavenago, P. Agostinetti, P. Sonato, and L. Zanotto, Rev. Sci. Instrum. 87, 02B305 (2016).

[14]M. Barbisan, C. Baltador, B. Zaniol, M. Cavenago, U. Fantz, R. Pasqualotto, G. Serianni, L. Vialetto, and D. Wünderlich, Rev. Sci. Instrum. 87, 02B319 (2016).

[15]K. Behringer and U. Fantz, J. Phys. D: Appl. Phys. 27, 2128 (1994).

[16]M. Tuszewski, Phys. Plasmas 5, 1198 (1998).